Ecología Austral 32:835-848 Diciembre 2022
Asociación Argentina de Ecología
https://doi.org/10.25260/EA.22.32.3.0.1812

Phytoplankton DNA metabarcoding in four sectors of the SW Atlantic in the context of the global ocean

Federico M. Ibarbalz[1,2,3,4,5,✉]; Juan J. Pierella Karlusich[5,6,9]; Sergio Velasco Ayuso[1,2,3,8]; Natalia Visintini[1,2,3]; Lionel Guidi[6,7]; Chris Bowler[5,6] & Pedro Flombaum[2,3,4,8]

[1] *Universidad de Buenos Aires, Facultad de Ciencias Exactas y Naturales. Buenos Aires, Argentina.* [2] *CONICET-Universidad de Buenos Aires. Centro de Investigaciones del Mar y la Atmósfera (CIMA). Buenos Aires, Argentina.* [3] *Institut Franco-Argentin d'Études sur le Climat et ses Impacts, International Research Laboratory (IRL-IFAECI/CNRS-CONICET-UBA). Buenos Aires, Argentina.* [4] *Instituto Universitario de Seguridad Marítima, Prefectura Naval Argentina. Buenos Aires, Argentina.* [5] *Institut de Biologie de l'École Normale Supérieure (IBENS), Département de Biologie, École Normale Supérieure, CNRS, INSERM, Université de Recherche Paris Sciences et Lettres (Université PSL). Paris, France.* [6] *Research Federation for the Study of Global Ocean Systems Ecology and Evolution, FR2022/Tara GOSEE, Paris, France.* [7] *Sorbonne Université, Centre National de la Recherche Scientifique, Laboratoire d'Océanographie de Villefranche (LOV), Villefranche-sur-Mer, France.* [8] *Universidad de Buenos Aires, Facultad de Ciencias Exactas y Naturales, Departamento de Ecología Genética y Evolución. Buenos Aires, Argentina.*[9] *FAS Division of Science, Harvard University, Cambridge, MA.*

Abstract. The Southwest Atlantic Ocean (SWAO) is a spatially dynamic region with a remarkably high primary productivity. An exhaustive identification of the members of its phytoplankton community is a key step to understand the processes that sustain this ecosystem. Here, we provide a community composition analysis of eukaryotic phytoplankton in four SWAO sectors. We gathered 18S rRNA gene metabarcoding data and complemented it with confocal microscopy images, both from the *Tara* Oceans expedition in late spring 2010. Our work showed local and regional variation across three different size fractions that reflect the complexity of this region. Diversity decreased along temperature and latitudinal gradients, but also showed intricate patterns of occurrences across samples, suggesting that multiple factors shape the community structure. Samples resembled communities from other temperate regions and showed an increasing influence by cold waters from the Southern Ocean towards higher latitudes. These results complement previous regional studies that used other methods such as microscopy or pigment analysis. Our study contributes to the beginning of genomic-based surveys of plankton communities in the SW Atlantic and calls for further work in the region to enhance ecosystem monitoring and projections in the context of global change.

[Keywords: diatoms, dinoflagellates, primary productivity, biodiversity, 18S rRNA gene]

Resumen. Análisis de *metabarcoding* de ADN para el fitoplancton en cuatro sectores del Atlántico Suroeste en el contexto del océano global. El Océano Atlántico Suroeste es una región espacialmente dinámica, con sectores de alta productividad primaria. Un paso fundamental en la comprensión de los procesos que sostienen este ecosistema consiste en identificar a las especies del fitoplancton de forma exhaustiva. En el presente estudio analizamos la composición de la comunidad del fitoplancton eucariota en cuatro sectores del Océano Atlántico Suroeste. Para ello utilizamos datos de secuenciación masiva del gen ARNr 18S e imágenes de microscopía confocal de la expedición *Tara* Oceans, correspondientes a la primavera tardía del 2010. Las variaciones locales y regionales en las tres fracciones de tamaño que analizamos reflejan la complejidad de este ecosistema. Mientras la diversidad disminuyó hacia altas latitudes y bajas temperaturas, la comunidad presentó patrones intrincados en la composición de sus muestras, lo que sugiere la existencia de múltiples factores que determinan la estructura de la comunidad. Las muestras se asemejaron a las comunidades de otras regiones oceánicas templadas del planeta, aunque con una influencia de las aguas frías del Océano Antártico en el caso de las más australes. Estos resultados complementan estudios regionales previos en los que se utilizaron otros métodos como la microscopía o el análisis de pigmentos. Nuestro trabajo contribuye al comienzo de estudios genómicos de las comunidades de plancton en el Atlántico Suroeste y resalta la necesidad de contar con más estudios en la región para mejorar el monitoreo y las proyecciones de los ecosistemas en el contexto del cambio global.

[Palabras clave: diatomeas, dinoflagelados, productividad primaria, biodiversidad, gen ARNr 18S]

Editor asociado: Pedro Daleo
✉ federico.ibarbalz@cima.fcen.uba.ar
Recibido: 24 de Septiembre de 2021
Aceptado: 29 de Abril de 2022

Introduction

The southwest region of the Atlantic Ocean (SWAO) exhibits remarkable levels of annual primary production that sustain important fisheries and promote a major export of carbon (Yoder and Kennelly 2003; Bianchi et al. 2009; Guidi et al. 2016). The region features a sharp contrast in water masses due to the confluence of warm subtropical waters from the Brazil current (>18 °C and salinity >36) (Campos et al. 1995) with the colder waters (<15 °C and salinity <34.2) of the Malvinas current (Piola and Gordon 1989). It also exhibits a permanent thermohaline shelf-break front off Argentina, where subantarctic shelf-waters join with cooler and saltier waters from the Malvinas current (Acha et al. 2004; Brun et al. 2020). Shelf waters are modulated by low salinity waters from the discharge of Magallanes and Le Maire straits. In this diversity of conditions at temperate latitudes, marine phytoplankton thrive (Carreto et al. 1995; Gayoso and Podestá 1996; Acha et al. 2004).

Phytoplankton communities can be assembled locally 1) through members that are advected (dispersal from the south by the Malvinas current), 2) through members that are selected by the imposed environmental conditions (ecological selection, nutrient concentration), 3) through random processes (ecological drift), or 4) by a combination of some or all of these mechanisms (Nemergut et al. 2013). Deciphering the assembly process in a particular oceanic region is never straightforward, mainly due to the dynamic complexity of the system and the large spatial scale usually involved (Sommeria-Klein et al. 2021). Improving our understanding of the phytoplankton community composition is a necessary first step.

Efforts to assess the phytoplankton community of the SWAO have included various complementary approaches (Hoffmeyer et al. 2018). Pigment analysis through high-performance liquid chromatography (HPLC) revealed the regional prevalence of diatoms and, to a lesser extent, dinoflagellates (Moreno et al. 2012). Optical determinations identified the influence of fronts on phytoplankton blooms at the Brazil-Malvinas confluence (Gayoso and Podestá 1996), as well as clear latitudinal variations in diatoms along temperature gradients, despite high interannual variability (Olguin Salinas et al. 2015a, 2015b). Additionally, various *in situ* measurements and satellite-based detection of ocean color patterns and mesoscale features indicated the seasonal presence of huge numbers of coccolithophores along the upper shelf-break (d'Ovidio et al. 2010; Segura et al. 2013; Balch et al. 2014). Furthermore, depending on the studied subregion, a seasonal succession from diatoms to coccolithophores is often observed (Gonçalves-Araujo et al. 2016). To our knowledge, molecular surveys based on next-generation sequencing of DNA to study the entire community have not been performed yet. High-throughput DNA sequencing significantly increases the resolution at which the community composition is studied, which may be particularly important for the smallest organisms that cannot be easily identified by light microscopy. Moreover, extending studies into the rare, less abundant members of the ecosystem could represent a valuable complement to previous plankton surveys in this oceanic sector.

The *Tara* Oceans expedition (Karsenti et al. 2011) sailed across the major oceanic basins between 2009 and 2013 to study plankton communities with state-of-the-art methodologies. Using standardized protocols, the expedition took samples in different water layers, and for a wide range of plankton organism sizes, in combination with a detailed contextual description (Pierella Karlusich et al. 2020; Sunagawa et al. 2020). Here, we analysed the eukaryotic phytoplankton community of the SWAO using *Tara* Oceans data mainly derived from 18S rRNA gene metabarcoding. In particular, we explored phytoplankton community composition and diversity within three different size fractions and two distinct water layers in the context of biotic and abiotic factors. We complemented the molecular observations with images from confocal microscopy. We then compared the community composition with that of samples from the global ocean. Overall, this study intends to shed light on the process of marine phytoplankton community assembly in the SWAO. Specifically, it offers a knowledge base for future omics surveys of marine microorganisms in this region of the ocean.

Materials and Methods

In the late spring of 2010 (29th November-16th December), the *Tara* Oceans expedition sailed from Buenos Aires to Ushuaia (Argentina) onboard the oceanographic schooner TARA and sampled at four different stations of the

SWAO. During this leg, the expedition aimed at stations in the center of relatively stable oceanic features (e.g., an eddy or a major current). For this, preliminary locations were selected on a sea surface height map about a week prior to the sampling. The four definitive stations were located between 40° S and 55° S (Figure 1A). A complete physical data report by station can be found in store.pangaea.de/Projects/TARA-OCEANS/Station_Reports/. Station TARA_080 (29th November) was located in an area dominated by mesoscale features. Temperature and salinity fell within the range of the subtropical waters, which were part of an anticyclonic structure originated from the Brazil-Malvinas confluence (Valla et al. 2018). Station TARA_081 (2nd December) was located in a well-mixed cooler water mass within a transition area between subtropical and subpolar waters. Station TARA_082 (7th December) was planned to sample the community associated with the cold Malvinas current. Station TARA_083 (16th December) was located at the southern end of the continental shelf before sailing across the Le Maire Strait, in an area known as Patagonian cold estuarine zone where low-salinity waters from the Pacific enter the Atlantic (Acha et al. 2004). Samples belong to the epipelagic/photic layer, namely to the surface (SRF, ≤5 m) and the deep-chlorophyll maximum (DCM), with variable depths for each station (39-60 m) (Table 1), except for station TARA_083, that was performed with a fast sampling scheme focused on the surface due to time constraints of the global expedition.

The environmental conditions were recorded at each station. Detailed protocols from the *Tara* Oceans expedition can be found in Pesant et al. (2015), and full contextual data are available at doi.org/10.1594/PANGAEA.875582. Water temperature was measured with a vertical profile sampling system (CTD-rosette). Chlorophyll a (chl a) concentrations were obtained through HPLC (Van Heukelem and Thomas 2001; Ras et al. 2008). Nitrate (NO_3^-) ions were analysed according to the protocol of Bendschneider and Robinson (1952). Total water column depth was obtained from the American Oceanic and Atmospheric Administration (NOAA) via R-package marmap (version 1.0.5) (Pante and Simon-Bouhet 2013) specifically for this work. We included abundances of other broad planktonic groups to further characterize each sample habitat. Large planktonic organisms were collected with different nets that were towed vertically from 500 m to the surface. Here, we constrained it to copepod counts from the WP2 net (mesh size of 200 µm) (EcoTaxa) (EcoTaxa; ecotaxa.obs-vlfr.fr/prj/377, ecotaxa.obs-vlfr.fr/prj/378). Abundances of picoplankton groups (composed mainly

Table 1. Eukaryotic phytoplankton diversity in the SW Atlantic Ocean. The table represents latitude and longitude (lat/lon), surface (SRF, <5m) and deep-chlorophyll maximum (DCM, depth in brackets) sampled depth layers, and diversity of the phytoplankton community at each station derived from 18S rRNA gene metabarcoding. '# of observed tax. categ.' refers to the number of non-duplicated eukaryotic taxonomies for each size fraction (expressed in µm). The exponential Shannon index [exp(H')] represents an estimate of the effective number of species. The last two rows represent the mean (and standard deviation).

Tabla 1. Diversidad de fitoplancton eucariota en el Océano Atlántico Suroeste. La tabla representa la latitud y longitud (lat/lon), las capas de profundidad muestreadas con la superficie (SRF, <5 m) y el máximo de clorofila profunda (DCM, profundidad entre paréntesis), y la diversidad de la comunidad de fitoplancton en cada estación en base a datos de metabarcoding del gen ARNr 18S. '# of observed tax. categ.' se refiere a taxonomías eucariotas no duplicadas para cada fracción de tamaño (expresado en µm). El índice de Shannon exponencial [exp (H')] representa una estimación del número efectivo de especies. Las dos últimas filas representan la media (y la desviación estándar).

Tara Oceans station	lat/lon [°S/W]	Water column [m]	Sampled layer	# of observed tax. categ.			exp(H')		
				0.8-5 µm	5-20 µm	20-180 µm	0.8-5 µm	5-20 µm	20-180 µm
080	40.6/51.1	5539	SRF	253	-	143	70	-	29
	40.6/51.9	5696	DCM (60 m)	259	166	163	50	54	50
081	44.5/52.5	5909	SRF	197	151	133	50	18	15
	44.5/52.2	5925	DCM (39 m)	203	124	86	43	12	8
082	47.2/58.2	3066	SRF	181	125	119	25	6	6
	47.2/57.9	3684	DCM (42 m)	175	92	-	22	12	-
083	54.4/65.1	92	SRF	172	126	115	39	8	8
All	-		SRF	201 (36)	134 (13)	128 (15)	46 (19)	11 (7)	14 (10)
All	-		DCM	212 (43)	127 (37)	124 (54)	39 (14)	26 (24)	29 (30)

of bacterioplankton) were determined by flow cytometry (data.mendeley.com/datasets/p9r9wttjkm/2; Hingamp et al. 2013; Sunagawa et al. 2015). Relative abundances of N_2-fixers (or diazotrophs) were obtained from (Pierella Karlusich et al. 2020) and correspond to the values generated by metagenomic read mapping against a comprehensive sequence database of the marker gene for diazotrophs, *nifH*, and a marker gene for bacteria, *recA*.

The eukaryotic plankton community composition at each station was determined using 18S rRNA gene metabarcoding through high-throughput Illumina sequencing. For this procedure, DNA was extracted from size-fractionated samples (0.8-5 μm, 5-20 μm, and 20-180 μm; pico-nano, nano and micro, respectively) (Pesant et al. 2015) and analysed by amplicon-sequencing of the V9 region from the 18S rRNA gene (Alberti et al. 2017). Reads were processed into operational taxonomic units (OTUs; a proxy for species in DNA-based surveys) obtained through the swarms method (Mahé et al. 2014), and classified taxonomically against a customized ribosomal reference database (for complete details see de Vargas et al. (2015) and its companion website taraoceans.sb-roscoff.fr/EukDiv/; the global OTU table is available at zenodo.org/record/3768510). Photosynthetic unicellular eukaryotes were identified based on their taxonomic affiliation, and only those with >80% identity with the database reference sequences were kept. We included photosynthetic dinoflagellates when their taxonomic resolution was sufficient to match known photosynthetic lineages from the literature. We did not include mixotrophs that obtain their chloroplast or photosynthetic capacity by different mechanisms from other unicellular organisms (Pierella Karlusich et al. 2020). Throughout this work we refer to deep-branch lineages that consist of a set of informative names of phyla (e.g., Bacillariophyta) and classes (e.g., Dinophyceae) within eukaryotic phytoplankton. A table for the top-100 phytoplankton OTUs of the SWAO is available in Appendix 1 (doi.org/10.17632/ppbhwn3bcy.1).

As a measure of diversity we included both the exponential Shannon index (exp[H'], an estimate for the effective number of species) and the number of observed taxonomic categories (i.e., two OTUs with equal taxonomic classification count as one taxonomic category). We chose the latter over the plain number of OTUs as a more conservative estimate. Multivariate analyses (i.e., clustering and ordination) were performed on the OTU table. We used the R-package vegan (version 2.5-4) (Oksanen et al. 2019) to calculate Bray-Curtis dissimilarities with the function vegdist both in default mode (on Hellinger-transformed compositional data) and in binary mode (binary=T; i.e., presence/absence). The principal coordinates analysis was carried out via the function wcmdscale on the global dissimilarity matrix derived from the Hellinger-transformed compositional data and only the two first axes were displayed. We set focus on the two major basins (Atlantic and Pacific, north-south) and the Southern Ocean to follow the main analysis in Ibarbalz et al. (2019) and without the Arctic samples due to differences in size fractions. By compositional data we refer to abundances relativized by the total number of phytoplankton reads per sample. The R-function hclust served for performing the hierarchical clustering analysis, using the unweighted average linkage criterion.

Finally, to further support the observations derived from 18S rRNA gene metabarcoding, we inspected the *Tara* Oceans dataset of environmental High Content Fluorescence Microscopy (eHCFM) (Colin et al. 2017) from samples corresponding to size fractions 5-20 μm and 20-180 μm (ebi.ac.uk/biostudies/studies/S-BSST51 and ecotaxa.obs-vlfr.fr/prj/2274) using the Ecotaxa web platform (Picheral et al. 2017).

Results

In the SWAO, eukaryotic phytoplankton comprised 445 taxonomic categories, from which 347 (78%) corresponded to the genus level. This taxonomic diversity decreased from small to large size fractions, both at high and low taxonomic levels (Table 1). The pico-nano fraction (i.e., 0.8-5 μm) had several lineages well represented in all sampling sites, with diatoms (Bacillariophyta), dinoflagellates (Dinophyceae), dictyochophytes, haptophytes, cryptophytes and the chlorophytes Mamiellophyceae as major constituents (Figure 1). The micro fraction (i.e., 20-180 μm) had mostly two dominant groups, diatoms and dinoflagellates, and the nano fraction (i.e., 5-20 μm) had intermediate levels of taxonomic diversity (Table 1). Further differences can be illustrated at the level of OTUs, such as with the dominance of small-sized representants of the genera *Aureococcus* (Pelagophyceae) and *Florenciella* (Dictyochophyceae) in the pico-

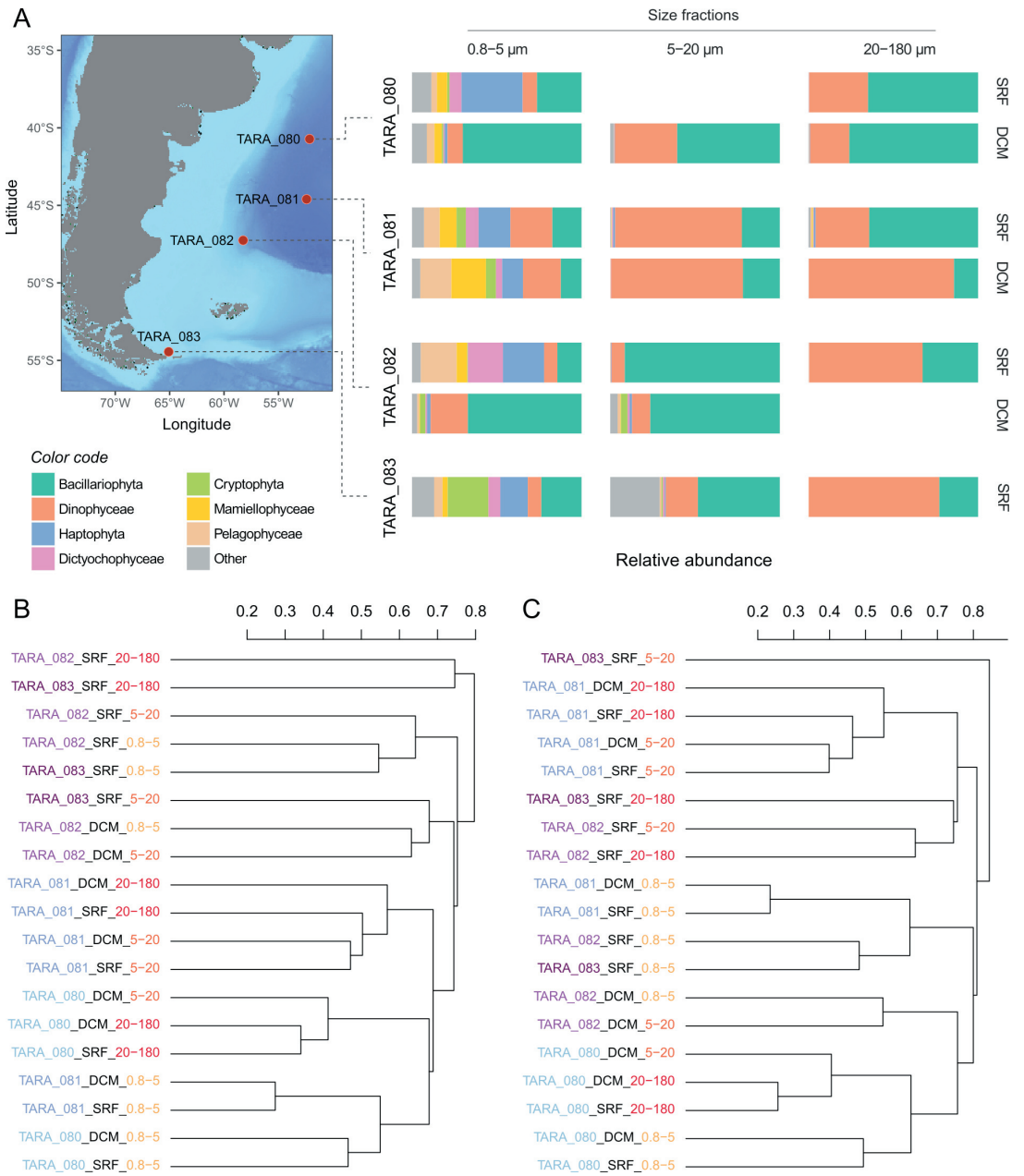

Figure 1. Eukaryotic phytoplankton community composition in the SW Atlantic Ocean. (A) On the left, locations of the four stations from the *Tara* Oceans expedition in the late austral spring of 2010. Bathymetry is represented on a scale from light blue (continental shelf) to dark blue (open ocean). On the right, the relative abundance for main eukaryotic phytoplankton deep-branch lineages identified through 18S rRNA gene metabarcoding for each station, depth layer (surface, SRF; deep-chlorophyll maximum, DCM), and size fractions obtained with the use of filters with different mesh size. (B/C) Hierarchical clustering analysis (unweighted average linkage) based on Bray-Curtis dissimilarities (see scales). Calculation was done based on (B) presence/absence of eukaryotic phytoplankton and (C) their compositional data or proportions (see Materials and Methods).

Figura 1. Composición de la comunidad de fitoplancton eucariota en el Océano Atlántico Suroeste. (A) A la izquierda, las ubicaciones de las cuatro estaciones de la expedición *Tara* Oceans en la primavera tardía austral de 2010. La batimetría está representada en una escala de azul claro (plataforma continental) a azul oscuro (océano abierto). A la derecha, la abundancia relativa de los principales linajes eucariotas del fitoplancton identificados mediante *metabarcoding* del gen 18S rRNA para cada estación, capa de profundidad (superficie, SRF; máximo de clorofila profunda, DCM) y fracciones de tamaño obtenidas con el uso de filtros con diferente tamaño de poro. (B/C) Análisis de agrupamiento jerárquico (vínculo promedio no ponderado) basado en las diferencias de Bray-Curtis (ver escalas). El cálculo se realizó en base a (B) presencia/ausencia de fitoplancton eucariota y (C) sus datos de composición o proporciones (ver Materials and Methods).

nano fraction, in contrast with large-sized examples such as *Neoceratium* (Dinophyceae) and *Chaetoceros* (Bacillariophyta) among the OTUs of the 'micro' fraction (Appendix 1).

We observed contrasting patterns among the size fractions and the two water column features (i.e., SRF and DCM) (Figure 1A). The proportions of deep-branch lineages of the pico-nano size fraction were different between SRF and DCM in stratified waters (stations TARA_080 and TARA_082), but were similar in the station that presented an intense mixing (station TARA_081; Figure 1A). Similarly, the fraction of shared OTUs between SRF and DCM was lower in the stratified samples (stations TARA_080 and TARA_082, 36.61% and 14.29%, respectively) than in the intensely mixed station (TARA_081, 57.1%). The nano size fraction followed a similar trend with the stations TARA_082 and the well-mixed TARA_081 sharing 9.44% and 35.98% of OTUs between SRF and DCM, respectively. However, at the class/phylum level, community differences were less obvious (Figure 1A). On the contrary, communities of the micro size fraction were more similar in stratified waters between SRF and DCM (station TARA_080, 48.92% of shared OTUs) but differed in the well mixed station (station TARA_081, 32.63% of shared OTUs). Thus, although limited in the number of samples, our results show diverging patterns among size fractions and sample depths.

Eukaryotic phytoplankton community alpha- and beta-diversity exhibited regional patterns together with a latitudinal variation in temperature and concentration of chlorophyll a. We observed that the diversity of phytoplankton decreased with latitude and chlorophyll a, but increased with temperature (Table 1, Table 2). From north to south, surface chlorophyll a increased 2.4 times along the 13.8° transect. The same gradient showed a temperature decrease of 12.8 °C, accompanied by a reduction of 20-32% in taxonomic categories, and of 44-85% in the exponential Shannon diversity index, depending on the size fraction (Table 1, Table 2). A hierarchical clustering analysis based on presence/absence of OTUs resulted in a consistent north/south separation (i.e., stations TARA_080-081 vs TARA_082-083, irrespective of size fraction or water column layer) (Figure 1B), reflecting in part the loss in richness. The same analysis but based on OTU proportions resulted in a clustering by size rather than by sampling site (Figure 1C). The clustering by size suggested that a suite of OTUs were better represented in TARA_081, TARA_082 and TARA_083 compared to the most northern site (TARA_080) (Supplementary Material-Figure S1C). For example, an OTU belonging to the genus *Pycnococcus*, a small-sized group from the prasinophytes (Chlorophyta), was abundant only at station TARA_080 in the pico-nano size fraction, while the pelagophyte *Aureococcus anophagefferens* and the dinoflagellate *Gonyaulax spinifera* were more conspicuous in the three more southern surface samples. However, a wide variety of patterns can be found. For instance, OTUs assigned to *Pseudo-nitzschia delicatissima*

Table 2. Environmental variability in the SW Atlantic Ocean. The table represents surface (SRF, <5m) and deep-chlorophyll maximum (DCM, depth in brackets) sampled depth layers, nitrate concentration, salinity, water temperature, and concentration of chlorophyll a (Chl a). The last two rows represent the mean (and standard deviation).

Tabla 2. Variabilidad ambiental en el Océano Atlántico Suroeste. La tabla representa las capas de profundidad muestreadas con la superficie (SRF, <5 m) y el máximo de clorofila profundo (DCM, profundidad entre paréntesis), la concentración de nitrato, la salinidad, la temperatura del agua (Water temperature), y la concentración de clorofila *a* (Chl a). Las dos últimas filas representan la media (y la desviación estándar).

Tara Oceans station	Sampled layer	NO_3^- [µmol/L]	Salinity	Water temperature [°C]	Chl a [mg/m^3]
080	SRF	ND	35.62	19.93	0.13
	DCM (60 m)	0.83	35.81	17.79	0.20
081	SRF	2.44	34.79	13.68	0.23
	DCM (39 m)	2.81	34.81	13.51	0.29
082	SRF	18.43	34.05	7.58	0.43
	DCM (42 m)	18.05	34.05	7.15	0.51
083	SRF	13.59	33.25	7.13	0.31
All	SRF	-	34.43 (1.01)	12.08 (6.03)	0.28 (0.13)
All	DCM	7.23 (9.42)	34.89 (0.88)	12.82 (5.35)	0.33 (0.16)

largely contribute to the two northern samples but not to those from the south. The diatoms *Thalassiosira tumida* and *Corethron inerme* were very well represented in the microplankton size fraction from the Malvinas current but not in the other sampling stations. Overall, OTU community composition revealed stronger regional diversity patterns than OTU dominance structure.

We were able to validate many OTU taxonomies when looking at the *Tara* Oceans

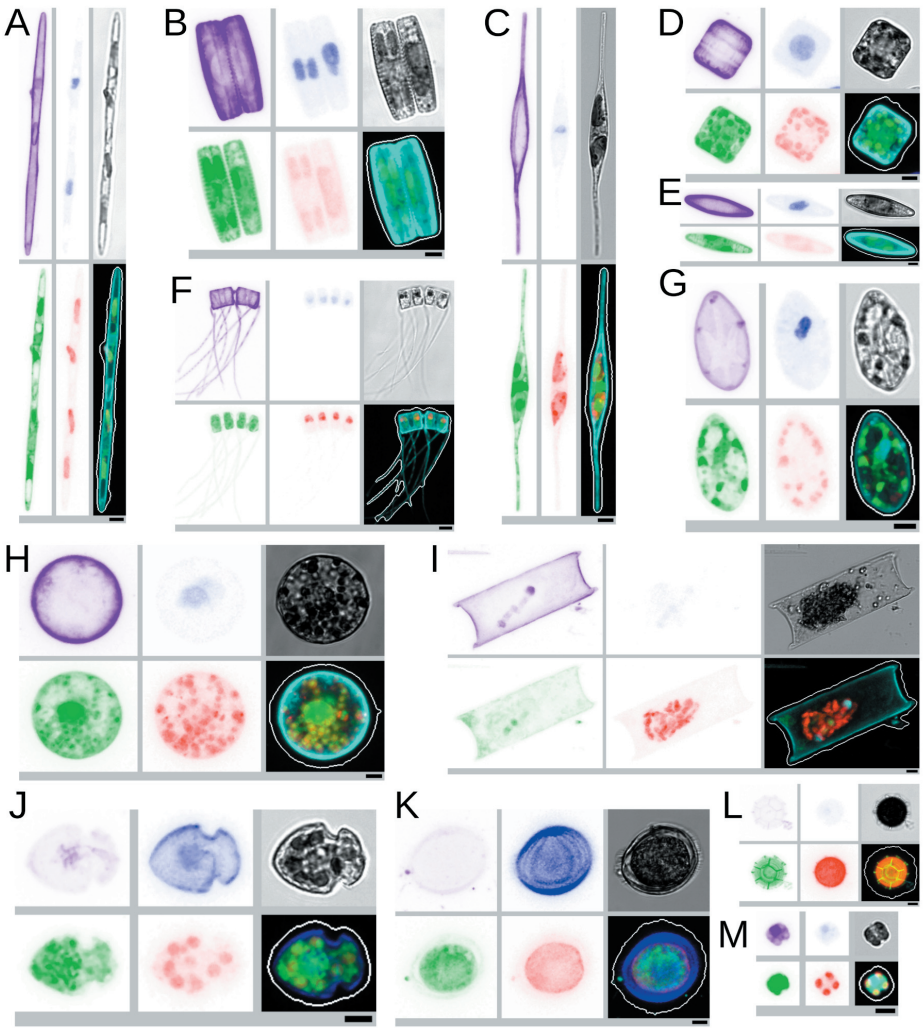

Figure 2. Microscopy observations of eukaryotic phytoplankton in *Tara* Oceans samples of the SW Atlantic Ocean. Images were obtained by environmental high content fluorescence microscopy (eHCFM) (Colin et al. 2017). From left to right, the displayed channels for each micrograph correspond to cell surface (cyan, AlexaFluor 546), cellular membranes (green, DiOC6), chlorophyll autofluorescence (red), the bright field, and the merged channels. The size bar at the bottom right of each panel corresponds to 2.5 µm. TARA_80 surface 20-180 µm: I (diatom *Hemiaulus* with a filament of the N_2-fixer cyanobacterium *Richelia*); TARA_81 DCM 5-20 µm: D (centric diatom), C and G (pennate diatoms), J (dinoflagellate, order Gonyaulacales), L (prasinophyte, genus *Pterosperma*); TARA_82 surface 5-20 µm: A, B and E (pennate diatoms), F (diatom, probably genus *Chaetoceros*), M (haptophyte, probably genus *Phaeocystis*); TARA_82 surface 20-180 µm: H (coscinodiscales), K (dinoflagellate).

Figura 2. Observaciones por microscopía de fitoplancton eucariota en muestras de *Tara* Oceans del Océano Atlántico Suroeste. Las imágenes se obtuvieron mediante microscopía de fluorescencia de alto contenido ambiental (Colin et al. 2017). De izquierda a derecha, los canales mostrados para cada micrografía corresponden a la superficie celular (cian, AlexaFluor 546), membranas celulares (verde, DiOC6), autofluorescencia de clorofila (rojo), el campo claro y los canales superpuestos. La barra de tamaño en la parte inferior derecha de cada panel corresponde a 2.5 µm. TARA_80 superficie 20-180 µm: I (diatomea *Hemiaulus* con un filamento de la cianobacteria *Richelia* fijadora de N2); TARA_81 máx. Chl a 5-20 µm: D (diatomea céntrica), C y G (diatomeas pennadas), J (dinoflagelados, orden Gonyaulacales), L (prasinofito, género *Pterosperma*); TARA_82 superficie 5-20 µm: A, B y E (diatomeas pennadas), F (diatomea, probablemente género *Chaetoceros*), M (haptofito, probablemente género *Phaeocystis*); TARA_82 superficie 20-180 µm: H (coscinodiscales), K (dinoflagelados).

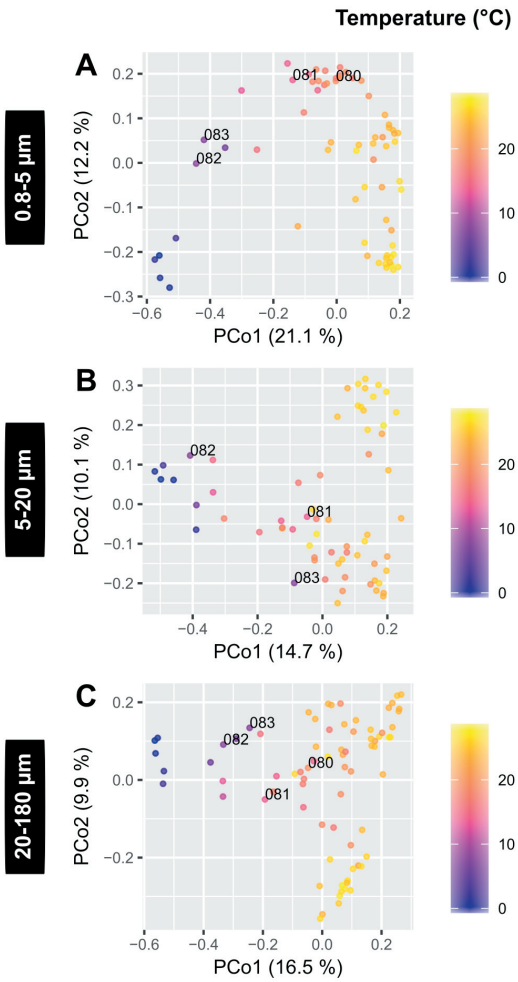

Figure 3. Eukaryotic phytoplankton community from the SW Atlantic Ocean in the context of the global ocean. Principal coordinates analysis performed on a Bray-Curtis dissimilarity matrix for phytoplankton communities of the sea surface. Each plot (A-C) corresponds to different size fractions. Only the first two ordination axes are shown, with their corresponding explained fraction of variance (%). Communities were inferred from 18S rRNA gene metabarcoding, and Bray-Curtis dissimilarity was calculated based on the Hellinger-transformed abundances previously normalised by the total phytoplankton reads per sample. Points corresponding to the four stations from the SW Atlantic analysed here have top-right labels. Color code represents sea surface temperature [°C]; see Supplementary Material-Figure S1 for color codes according to ocean basin and latitude.

Figura 3. Comunidad de fitoplancton eucariota del Océano Atlántico Suroeste en el contexto del océano global. Análisis de coordenadas principales realizado sobre una matriz de disimilitud de Bray-Curtis para comunidades de fitoplancton de la superficie del mar. Cada gráfico (A-C) corresponde a fracciones de diferente tamaño. Solo se muestran los dos primeros ejes de ordenación, con su correspondiente fracción de varianza explicada (%). Las comunidades se infirieron a partir de datos de *metabarcoding* del gen ARNr 18S, y la disimilitud de Bray-Curtis se calculó en base a las abundancias transformadas (Hellinger) previamente normalizadas por las lecturas de fitoplancton total por muestra. Los puntos correspondientes a las cuatro estaciones del Atlántico Suroeste analizadas aquí tienen rótulos en la parte superior derecha. El código de color representa la temperatura de la superficie del mar [°C]; consulte los códigos de color correspondientes a la cuenca oceánica y la latitud en Supplementary Material-Figure S1.

confocal microscopy dataset (Colin et al. 2017). We found images coming from the nano (5-20 µm) and micro (20-180 µm) size fractions assigned to diatoms, dinoflagellates, haptophytes and chlorophytes (Figure 2). Also, confocal microscopy allowed us to detect the symbiosis of a diatom (*Hemiaulus*) with a nitrogen-fixing cyanobacterium (*Richelia*) in station TARA_080 (Figure 2I). These results highlight the utility of complementing the molecular tools with microscopic observations that can further inform on cellular shapes, physiologies and ecological interactions.

The photosynthetic microbial composition of the SWAO resembled communities from the global ocean (Figure 3, Supplementary Material S1). Global marine eukaryotic phytoplankton communities from *Tara* Oceans ordinated broadly along a temperature gradient regardless of the size fraction (Figure 3A-C). Within this global ordination, the pico-nano (0.8-5 µm) and micro (20-180 µm) size fractions from SWAO presented similar and distinctive positions. The first position (stations TARA_082 and TARA_083) corresponded to a group with similarities to the Southern Ocean, together with a few specific samples from the South Pacific and North Atlantic Oceans. The second position (stations TARA_080 and TARA_081) was associated with a continuum from cold to warm waters from the Atlantic and Pacific Oceans (Supplementary Material-Figure S1A, C, E). This trend for the nano size fraction (5-20 µm) was slightly less pronounced since TARA_083 clustered closer to warmer stations and station TARA_080 was missing. Finally, all of them clustered far from the warmest stations near equatorial latitudes (Supplementary Material-Figure S1B, D, F).

Environmental abiotic and biotic conditions varied along the SW Atlantic leg of *Tara* Oceans (Table 2, Figure 4). Temperature dropped from almost 20 °C at the surface of station TARA_080, to around 7 °C in the station TARA_083 prior to Le Maire Strait (Table 2). Chlorophyll a ranged from 0.13 to 0.51 mg/

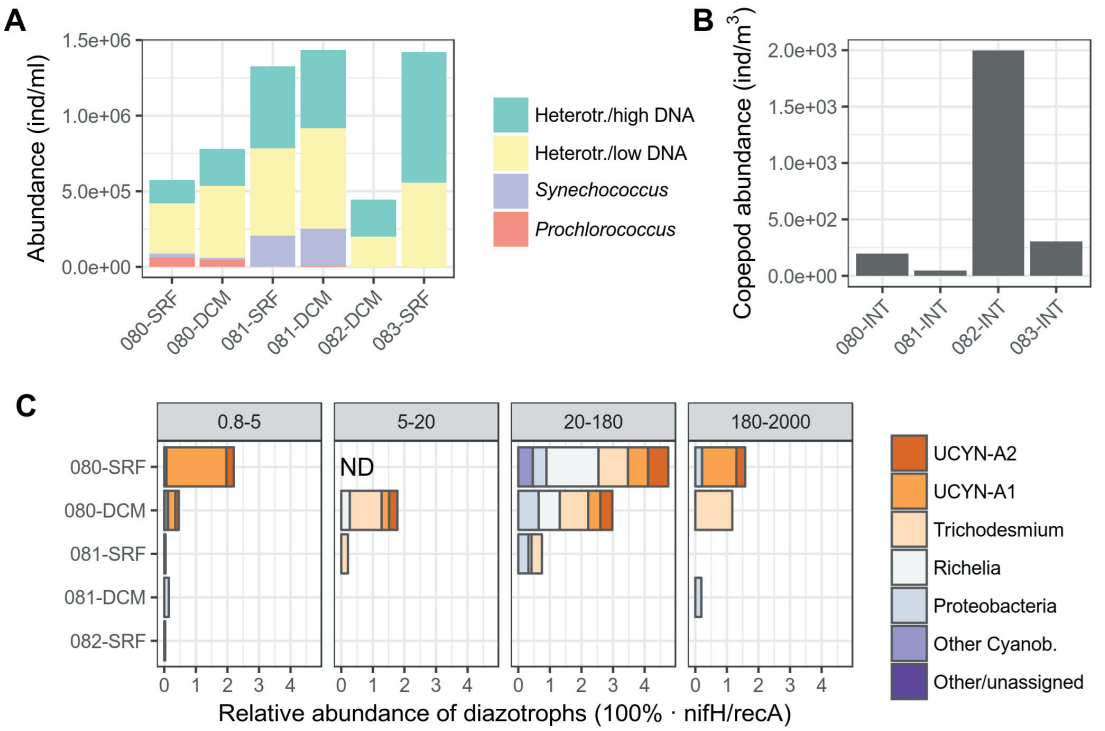

Figure 4. Abundances of other plankton groups in the SW Atlantic Ocean. (A) Flow cytometry cell counts for bacteria for each station and water layer (SRF, surface; DCM, deep-chlorophyll maximum). Heterotrophic organisms were of two types (high and low DNA content), and *Synechococcus* and *Prochlorococcus* refer to photosynthetic picocyanobacteria. (B) Copepod counts for each station integrated the water column from a depth of 500 m to the surface (INT; see Materials and Methods). (C) Relative abundances of bacterial diazotrophs in the metagenomes determined by normalizing read abundances corresponding to the *nifH* (nitrogenase) gene with those from the housekeeping gene *recA*. Station TARA_083 showed no detection for *nifH*.

Figura 4. Abundancia de otros grupos de plancton en el Océano Atlántico Suroeste. (A) Conteo de células por citometría de flujo para bacterias para cada estación y capa de agua (SRF, superficie; DCM profundidad del máximo de clorofila). Los organismos heterótrofos fueron de dos tipos (alto y bajo contenido de ADN), y *Synechococcus* y *Prochlorococcus* se refieren a picocianobacterias fotosintéticas. (B) Los conteos de copépodos para cada estación integraron la columna de agua desde una profundidad de 500 m hasta la superficie (INT; ver Materials and Methods). (C) Determinación de las abundancias relativas de diazótrofos bacterianos en los metagenomas mediante la normalización de las abundancias de lecturas correspondientes al gen *nifH* (nitrogenasa) con las del gen constitutivo *recA*. La estación TARA_083 no mostró detección de *nifH*.

m^3 at the surface of station TARA_080 and the DCM of station TARA_082, respectively (Table 2). The open-ocean nature of the first three stations versus the shallow conditions of station TARA_083 should also be noted (Table 2). Biotic conditions also varied widely, with differences in heterotrophic bacteria abundance ranging about one order of magnitude, and cyanobacteria being detected exclusively in the two warmest stations (TARA_080, TARA_081) (Figure 4A). The type of cyanobacteria varied in the same way as the nitrate concentration of the two warmest stations, with *Prochlorococcus* detected in the oligotrophic TARA_080 and *Synechococcus* in the nutrient-richer TARA_081 (Figure 4A, Table 2). Copepods peaked together with chlorophyll a in station TARA_082, where we observed a minimum of heterotrophic bacteria (Figure 4B). The comparison of abundances between copepod catches and molecular OTUs is however not straightforward due to differences in sampling protocols (500 m water column integration *vs.* punctual sampling, respectively; see Materials and Methods section), a fact that hinders a direct association between copepod abundances and grazing pressure. Finally, nitrate levels ranged from no detection in surface waters of TARA_080 to 18.0 µmol/L at TARA_082. TARA_080 showed a high abundance of N_2-fixers (diazotrophs), especially cyanobacterial symbionts of eukaryotic phytoplankton (Figure 4C). This included the *Richelia-Hemiaulus* symbiosis confirmed by microscopy (Figure 2I), as well as UCYN-A, which forms an endosymbiosis with a calcifying haptophyte closely related to *Braarudosphaera bigelowii* (Zehr et al.

2001). In the context of the global sampling, TARA_080 is among the few stations with high densities of UCYN-A (Pierella Karlusich et al. 2021). Altogether, these changes covaried consistently with those observed using DNA sequencing data of the 18S rRNA gene, suggesting important interactions between the eukaryotic phytoplankton community and the biotic and abiotic factors.

Discussion

DNA metabarcoding offers a complementary perspective on marine phytoplankton with respect to analyses based on remote sensing, microscopy or photosynthetic pigments via HPLC. Our depiction of broad phytoplankton groups through metabarcoding agrees with past studies, in which diatoms, dinoflagellates and haptophytes appeared as major groups of the temperate SWAO, especially around spring or early summer and offshore (Gibb et al. 2000; Aiken et al. 2009; Nunes et al. 2019). A further step was reached with the determination of taxa at the level of genus or species (Appendix 1) and their comparison with phytoplankton communities from other parts of the global ocean, revealing similarities between distant temperate waters. The lack of studies of inter-annual variability of phytoplankton communities in the area off the Patagonian shelf, the huge oceanographic variation of this region at the mesoscale, plus our limited number of samples hinders a more detailed comparison with past years. Additionally, a state-of-the-art microscopy imaging dataset and a precise metagenomic analysis aimed at the *nifH* gene helped us to point at symbioses between eukaryotic phytoplankton and nitrogen-fixing bacteria. Biological interactions involving phytoplankton are still being unveiled (e.g. Vincent et al. 2018) and for this, microscopic observations remain crucial (Pierella Karlusich et al. 2020). To our knowledge, the *Tara* Ocean samples represent the first 18S rRNA gene metabarcoding survey of the SWAO plankton in the vicinity of the Argentine Sea and, in spite of the limited number of samples, they provide relevant regional data.

The regional diversity that we found reflects latitudinal gradients observed for the SWAO for different microscopic organisms such as diatoms, tintinnids and copepods, with decreasing diversity in the poleward direction (Thompson 2004; Olguin Salinas et al. 2015a; Becker et al. 2021). This decrease in diversity was associated with temperature and ocean currents as driving factors (Olguin Salinas and Alder 2011; Olguin Salinas et al. 2015a). Additionally, it agrees with global phytoplankton diversity gradients reported recently (Ibarbalz et al. 2019; Righetti et al. 2019). Although restricted in number, the corresponding *Tara* Oceans samples coincided with these findings regardless of the size fraction of phytoplankton analyzed. The diversity of the smallest sized eukaryotic phytoplankton, reported previously for subregions or specific locations (Silva et al. 2009; Antacli et al. 2018), displayed a decreasing diversity pattern with latitude, suggesting that similar driving factors apply to this cell size category.

The abiotic and biotic parameters of the stations (Table 2, Figure 4) reflected the transition between Brazil and Malvinas currents and their broad trophic regimes. The Brazil current transports warm, oligotrophic water from the north, with limited input of deep-water nutrients into the euphotic layer due to low vertical mixing (Brandini et al. 2000). In these oligotrophic waters, productivity relies on nutrient input from mostly regenerated sources (Becker et al. 2021), cyanobacteria thrive (Flombaum et al. 2013), and nitrogen fixers presence and activity is favoured (Delmont et al. 2018). The Malvinas current consists of cold waters with higher concentration of nutrients, a condition that potentially allows new production, and where zooplankton abundances can be high (Figure 4B; Berasategui et al. 2005; Thompson et al. 2014). The genus *Prochlorococcus* becomes undetectable (Figure 4A) and eukaryotic representatives become the dominant phytoplankton groups (Pierella Karlusich et al. 2020). These trophic regimes are the result of a variety of ecological processes that we are only starting to decipher, and that the highly contrasting conditions that unfold in the SWAO may help to unveil.

Within the perspective of the extended *Tara* Oceans survey, the regional diversity observed here appears as part of a global, warm-cold continuum (Figure 3). The combined effect of environmental factors and advection is likely behind the similarity between the SWAO stations with others from temperate waters in neighboring oceans (Figure S1). Plankton's enormous populations are transported by currents, while temperature is a major community structuring force in the ocean

(Sunagawa et al. 2015; Ibarbalz et al. 2019; Righetti et al. 2019). Selection forcings act also as a major barrier for dispersal across basins, as it has been observed in the Agulhas rings carrying Indian Ocean waters across the Atlantic (Villar et al. 2015). The Brazil-Malvinas system displays stable eddies after the confluence that drift to the southeast (Legeckis and Gordon 1982), and this could offer a steeper gradient for studying these processes. Future metabarcoding surveys could build on this framework and on past studies that described the complex interplay between different water masses and biological interactions in this area (Gayoso and Podestá 1996; Gonçalves-Araujo et al. 2016). This could be especially important for complementing evidence that the confluence zone is moving southwards due to global change (Goni et al. 2011; Leyba et al. 2019).

The diversity of the largest size fraction does not necessarily reflect the diversity of the planktonic community as a whole. Species diversity varies across the phytoplankton size spectrum in a skewed log-normal manner, with a maximum at intermediate sizes, although alternative patterns have also been suggested (Finkel 2007). Our results showed a higher regional and local taxonomic variability for the pico-nano size fraction with respect to the nano and micro eukaryotic phytoplankton fractions (Figure 1, Table 1). At least two reasons may explain this difference. First, current metabarcoding protocols in combination with bioinformatic tools allow unravelling a great part of the diversity of the pico-nano phytoplankton size fraction that is more difficult to identify in traditional microscopic surveys (de Vargas et al. 2015; Malviya et al. 2016). Second, the simultaneous action of top-down (grazer abundance) and bottom-up (nutrient concentration) controls could promote differences in the relative distribution of large versus small cells through, for example, the tradeoff between nutrient acquisition and protection against predation (Smetacek 2001; Simon et al. 2009). Thus, DNA metabarcoding may reveal previously undetected controls of phytoplankton diversity in the SW Atlantic.

To conclude, the SWAO reveals itself as a highly diverse region in the global ocean. It combines high and low productive waters with temperate phytoplankton communities influenced by cold and warm waters. High-throughput sequencing data further support this idea, and highlight the potential of the region for natural experiments and gradient analyses that could provide relevant insights into the coupling of phytoplankton communities and their role in carbon export in the context of a changing ocean.

Acknowledgements. This work was written in the frame of a ECOS Sud bilateral project (AT08ST18) and supported by Assemble+ (PID8395), University of Buenos Aires (UBACYT20020170100620BA), ANPCyT (PICT 2017-3020) and Programa INVESTIGACIÓN, DESARROLLO E INNOVACIÓN EN CIENCIAS DEL MAR A6 BioMMAr. We thank Martin Saraceno and Viviana Alder for their help during the manuscript preparation. CB acknowledges funding from ERC Advanced Awards Diatomite and Diatomic, the FFEM - French Facility for Global Environment (Fonds Français pour l'Environnement Mondial) to JJPK, and the French Government "Investissements d'Avenir" Programmes MEMO LIFE (Grant ANR-10-LABX-54), Université de Recherche Paris Sciences et Lettres (PSL) (Grant ANR-1253 11-IDEX-0001-02), and OCEANOMICS Grant ANR-11-BTBR-0008. This article is contribution number 138 of *Tara* Oceans.

References

Acha, E. M., H. W. Mianzan, R. A. Guerrero, M. Favero, and J. Bava. 2004. Marine fronts at the continental shelves of austral South America: physical and ecological processes. Journal of Marine Systems 44:83-105. https://doi.org/10.1016/j.jmarsys.2003.09.005.

Aiken, J., Y. Pradhan, R. Barlow, S. Lavender, A. Poulton, P. Holligan, and N. Hardman-Mountford. 2009. Phytoplankton pigments and functional types in the Atlantic Ocean: A decadal assessment, 1995-2005. Deep Sea Research Part II: Topical Studies in Oceanography 56:899-917. https://doi.org/10.1016/j.dsr2.2008.09.017.

Alberti, A., J. Poulain, S. Engelen, K. Labadie, S. Romac, I. Ferrera, et al. 2017. Viral to metazoan marine plankton nucleotide sequences from the Tara Oceans expedition. Scientific Data 4. https://doi.org/10.1038/sdata.2017.93.

Antacli, J. C., R. I. Silva, A. J. Jaureguizar, D. R. Hernández, M. Mendiolar, M. E. Sabatini, and R. Akselman. 2018. Phytoplankton and protozooplankton on the southern Patagonian shelf (Argentina, 47°-55°S) in late summer: Potentially toxic species and community assemblage structure linked to environmental features. Journal of Sea Research 140:63-80. https://doi.org/10.1016/j.seares.2018.07.012.

Balch, W. M., D. T. Drapeau, B. C. Bowler, E. R. Lyczkowski, L. C. Lubelczyk, S. C. Painter, and A. J. Poulton. 2014.

Surface biological, chemical, and optical properties of the Patagonian Shelf coccolithophore bloom, the brightest waters of the Great Calcite Belt. Limnology and Oceanography 59:1715-1732. https://doi.org/10.4319/lo.2014.59.5.1715.

Becker, É. C., M. G. Mazzocchi, L. C. P. de Macedo-Soares, M. C. Brandão, and A. S. Freire. 2021. Latitudinal gradient of copepod functional diversity in the South Atlantic Ocean. Progress in Oceanography 199:102710. https://doi.org/10.1016/j.pocean.2021.102710.

Bendschneider, K., and R. J. Robinson. 1952. A new spectrophotometric method for the determination of nitrite in sea water. Journal of Marine Research 11:87-96.

Berasategui, A. D., F. C. Ramírez, and A. Schiariti. 2005. Patterns in diversity and community structure of epipelagic copepods from the Brazil-Malvinas Confluence area, south-western Atlantic. Journal of Marine Systems 56:309-316. https://doi.org/10.1016/j.jmarsys.2004.12.002.

Bianchi, A. A., D. R. Pino, H. G. I. Perlender, A. P. Osiroff, V. Segura, V. Lutz, M. L. Clara, C. F. Balestrini, and A. R. Piola. 2009. Annual balance and seasonal variability of sea-air CO2 fluxes in the Patagonia Sea: Their relationship with fronts and chlorophyll distribution. Journal of Geophysical Research: Oceans 114. https://doi.org/10.1029/2008JC004854.

Brandini, F. P., D. Boltovskoy, A. Piola, S. Kocmur, R. Röttgers, P. C. Abreu, and R. M. Lopes. 2000. Multiannual trends in fronts and distribution of nutrients and chlorophyll in the southwestern Atlantic (30-62 S). Deep Sea Research Part I: Oceanographic Research Papers 47:1015-1033. https://doi.org/10.1016/S0967-0637(99)00075-8.

Brun, A. A., N. Ramirez, O. Pizarro, and A. R. Piola. 2020. The role of the Magellan Strait on the southwest South Atlantic shelf. Estuarine, Coastal and Shelf Science 237:106661. https://doi.org/10.1016/j.ecss.2020.106661.

Campos, E. J. D., J. E. Gonçalves, and Y. Ikeda. 1995. Water mass characteristics and geostrophic circulation in the South Brazil Bight: Summer of 1991. Journal of Geophysical Research: Oceans 100:18537-18550. https://doi.org/10.1029/95JC01724.

Carreto, J., V. A. Lutz, M. O. Carignan, A. D. C. Colleoni, and S. G. De Marco. 1995. Hydrography and chlorophyll a in a transect from the coast to the shelf-break in the Argentinian Sea. Continental Shelf Research 15:315-336. https://doi.org/10.1016/0278-4343(94)E0001-3.

Colin, S., L. P. Coelho, S. Sunagawa, C. Bowler, E. Karsenti, P. Bork, R. Pepperkok, and C. de Vargas. 2017. Quantitative 3D-imaging for cell biology and ecology of environmental microbial eukaryotes. Elife 6:e26066. https://doi.org/10.7554/eLife.26066.

d'Ovidio, F., S. De Monte, S. Alvain, Y. Dandonneau, and M. Lévy. 2010. Fluid dynamical niches of phytoplankton types. Proceedings of the National Academy of Sciences 107:18366-18370. https://doi.org/10.1073/pnas.1004620107.

Delmont, T. O., C. Quince, A. Shaiber, Ö. C. Esen, S. T. Lee, M. S. Rappé, S. L. MacLellan, S. Lücker, and A. M. Eren. 2018. Nitrogen-fixing populations of Planctomycetes and Proteobacteria are abundant in surface ocean metagenomes. Nature Microbiology 3:804-813.https://doi.org/10.1038/s41564-018-0176-9.

de Vargas, C., S. Audic, N. Henry, J. Decelle, F. Mahé, et al. 2015. Eukaryotic plankton diversity in the sunlit ocean. Science 348:1261605(1:11).

Finkel, Z. V. 2007. Does Phytoplankton Cell Size Matter? The Evolution of Modern Marine Food Webs. Pp. 333-350 *in* P. G. Falkowski and A. H. Knoll (eds.). Evolution of Primary Producers in the Sea. Academic Press, Burlington. https://doi.org/10.1016/B978-012370518-1/50016-3.

Flombaum, P., J. L. Gallegos, R. A. Gordillo, J. Rincón, L. L. Zabala, N. Jiao, D. M. Karl, W. K. W. Li, M. W. Lomas, D. Veneziano, C. S. Vera, J. A Vrugt, and A. C. Martiny. 2013. Present and future global distributions of the marine Cyanobacteria Prochlorococcus and Synechococcus. Proceedings of the National Academy of Sciences 110:9824-9. https://doi.org/10.1073/pnas.1307701110.

Gayoso, A. M., and G. P. Podestá. 1996. Surface hydrography and phytoplankton of the Brazil-Malvinas currents confluence. Journal of Plankton Research 18:941-951. https://doi.org/10.1093/plankt/18.6.941.

Gibb, S. W., R. G. Barlow, D. G. Cummings, N. W. Rees, C. C. Trees, P. Holligan, and D. Suggett. 2000. Surface phytoplankton pigment distributions in the Atlantic Ocean: an assessment of basin scale variability between 50 N and 50 S. Progress in Oceanography 45:339-368. https://doi.org/10.1016/S0079-6611(00)00007-0.

Gonçalves-Araujo, R., M. S. de Souza, C. R. B. Mendes, V. M. Tavano, and C. A. E. Garcia. 2016. Seasonal change of phytoplankton (spring vs. summer) in the southern Patagonian shelf. Continental Shelf Research 124:142-152. https://doi.org/10.1016/j.csr.2016.03.023.

Goni, G. J., F. Bringas, and P. N. Dinezio. 2011. Observed low frequency variability of the Brazil Current front. Journal of Geophysical Research: Oceans 116. https://doi.org/10.1029/2011JC007198.

Guidi, L., S. Chaffron, L. Bittner, D. Eveillard, A. Larhlimi, S. Roux, Y. Darzi, S. Audic, L. Berline, J. Brum, L. P. Coelho, J. C. I. Espinoza, S. Malviya, S. Sunagawa, C. Dimier, S. Kandels-Lewis, M. Picheral, J. Poulain, S. Searson, T. O. Coordinators, L. Stemmann, F. Not, P. Hingamp, S. Speich, M. Follows, L. Karp-Boss, E. Boss, H. Ogata, S. Pesant, J. Weissenbach, P. Wincker, S. G. Acinas, P. Bork, C. de Vargas, D. Iudicone, M. B. Sullivan, J. Raes, E. Karsenti, C. Bowler, and G. Gorsky. 2016. Plankton networks driving carbon export in the oligotrophic ocean. Nature 532:465-470. https://doi.org/10.1038/nature16942.

Hingamp, P., N. Grimsley, S. G. Acinas, C. Clerissi, L. Subirana, J. Poulain, I. Ferrera, H. Sarmento, E. Villar, G. Lima-Mendez, K. Faust, S. Sunagawa, J.-M. Claverie, H. Moreau, Y. Desdevises, P. Bork, J. Raes, C. de Vargas, E. Karsenti, S. Kandels-Lewis, O. Jaillon, F. Not, S. Pesant, P. Wincker, and H. Ogata. 2013. Exploring nucleo-cytoplasmic large DNA viruses in Tara Oceans microbial metagenomes. The ISME journal 7:1678-1695. https://doi.org/10.1038/ismej.2013.59.

Hoffmeyer, M. S., M. E. Sabatini, F. P. Brandini, D. L. Calliari, and N. H. Santinelli. 2018. Plankton ecology of the Southwestern Atlantic: From the subtropical to the subantarctic Realm. https://doi.org/10.1007/978-3-319-77869-3.

Ibarbalz, F. M., N. Henry, M. C. Brandão, S. Martini, G. Busseni, et al. 2019. Global trends in marine plankton diversity across kingdoms of life. Cell 179:1084-1097. https://doi.org/10.1016/j.cell.2019.10.008.

Karsenti, E., S. G. Acinas, P. Bork, C. Bowler, C. De Vargas, J. Raes, M. Sullivan, D. Arendt, F. Benzoni, J.-M. Claverie, M. Follows, G. Gorsky, P. Hingamp, D. Iudicone, O. Jaillon, S. Kandels-Lewis, U. Krzic, F. Not, H. Ogata, S. Pesant, E. G. Reynaud, C. Sardet, M. E. Sieracki, S. Speich, D. Velayoudon, J. Weissenbach, P. Wincker, and T. O. Consortium. 2011. A holistic approach to marine eco-systems biology. PLoS Biol 9:e1001177. https://doi.org/10.1371/journal.pbio.1001177.

Legeckis, R., and A. L. Gordon. 1982. Satellite observations of the Brazil and Falkland currents- 1975 1976 and 1978. Deep Sea Research Part A, Oceanographic Research Papers 29:375-401. https://doi.org/10.1016/0198-0149(82)90101-7.

Leyba, I. M., S. A. Solman, and M. Saraceno. 2019. Trends in sea surface temperature and air-sea heat fluxes over the South Atlantic Ocean. Climate Dynamics 53:4141-4153. https://doi.org/10.1007/s00382-019-04777-2.

Mahé, F., T. Rognes, C. Quince, C. de Vargas, and M. Dunthorn. 2014. Swarm: robust and fast clustering method for amplicon-based studies. PeerJ 2:e593. https://doi.org/10.7717/peerj.593.

Malviya, S., E. Scalco, S. Audic, F. Vincent, A. Veluchamy, J. Poulain, P. Wincker, D. Iudicone, C. de Vargas, L. Bittner, A. Zingone, and C. Bowler. 2016. Insights into global diatom distribution and diversity in the world's ocean. Proceedings of the National Academy of Sciences 113:E1516-E1525. https://doi.org/10.1073/pnas.1509523113.

Moreno, D. V., J. P. Marrero, J. Morales, C. L. García, M. G. V. Úbeda, M. J. Rueda, and O. Llinás. 2012. Phytoplankton functional community structure in Argentinian continental shelf determined by HPLC pigment signatures. Estuarine, Coastal and Shelf Science 100:72-81. https://doi.org/10.1016/j.ecss.2012.01.007.

Nemergut, D. R., S. K. Schmidt, T. Fukami, S. P. O'Neill, T. M. Bilinski, L. F. Stanish, J. E. Knelman, J. L. Darcy, R. C. Lynch, P. Wickey, and S. Ferrenberg. 2013. Patterns and processes of microbial community assembly. Microbiology and Molecular Biology Reviews 77:342-356. https://doi.org/10.1128/MMBR.00051-12.

Nunes, S., G. Pérez, M. Latasa, M. Zamanillo, M. Delgado, E. Ortega Retuerta, C. Marrasé, R. Simó, and M. Estrada. 2019. Size fractionation, chemotaxonomic groups and bio-optical properties of phytoplankton along a transect from the Mediterranean Sea to the SW Atlantic Ocean Sdena. Scientia Marina 83:87-109. https://doi.org/10.3989/scimar.04866.10A.

Oksanen, J., F. G. Blanchet, M. Friendly, R. Kindt, P. Legendre, D. McGlinn, P. R. Minchin, R. B. O'Hara, G. L. Simpson, P. Solymos, M. H. H. Stevens, E. Szoecs, and H. Wagner. 2019. vegan: Community Ecology Package. R package version 2.5-4.

Olguin Salinas, H. F., and V. A. Alder. 2011. Species composition and biogeography of diatoms in antarctic and subantarctic (Argentine shelf) waters (37-76 S). Deep Sea Research Part II: Topical Studies in Oceanography 58:139-152. https://doi.org/10.1016/j.dsr2.2010.09.031.

Olguin Salinas, H. F., V. A. Alder, A. Puig, and D. Boltovskoy. 2015a. Latitudinal diversity patterns of diatoms in the Southwestern Atlantic and Antarctic waters. Journal of Plankton Research 37:659-665. https://doi.org/10.1093/plankt/fbv042.

Olguin Salinas, H. F., F. Brandini, and D. Boltovskoy. 2015b. Latitudinal patterns and interannual variations of spring phytoplankton in relation to hydrographic conditions of the southwestern Atlantic Ocean (34-62 S). Helgoland Marine Research 69:177-192. https://doi.org/10.1007/s10152-015-0427-6.

Pante, E., and B. Simon-Bouhet. 2013. marmap: A Package for Importing, Plotting and Analyzing Bathymetric and Topographic Data in R. PLoS ONE 8. https://doi.org/10.1371/journal.pone.0073051.

Pesant, S., F. Not, M. Picheral, S. Kandels-Lewis, N. Le Bescot, G. Gorsky, D. Iudicone, E. Karsenti, S. Speich, R. Troublé, C. Dimier, and S. Searson. 2015. Open science resources for the discovery and analysis of Tara Oceans data. Scientific Data 2:150023. https://doi.org/10.1038/sdata.2015.23.

Picheral, M., S. Colin, and J.-O. Irisson. 2017. EcoTaxa, a tool for the taxonomic classification of images. URL: ecotaxa.obs-vlfr.fr.

Pierella Karlusich, J. J., F. M. Ibarbalz, and C. Bowler. 2020. Phytoplankton in the Tara Ocean. Annual Review of Marine Science 12:233-265. https://doi.org/10.1146/annurev-marine-010419-010706.

Pierella Karlusich, J. J., E. Pelletier, F. Lombard, M. Carsique, E. Dvorak, S. Colin, M. Picheral, F. M. Cornejo-Castillo, S. G. Acinas, R. Pepperkok, E. Karsenti, C. de Vargas, P. Wincker, C. Bowler, and R. A. Foster. 2021. Global distribution patterns of marine nitrogen-fixers by imaging and molecular methods. Nature Communications 12:1-18. https://doi.org/10.1038/s41467-021-24299-y.

Piola, A. R., and A. L. Gordon. 1989. Intermediate waters in the southwest South Atlantic. Deep Sea Research Part A. Oceanographic Research Papers 36:1-16. https://doi.org/10.1016/0198-0149(89)90015-0.

Ras, J., H. Claustre, and J. Uitz. 2008. Spatial variability of phytoplankton pigment distributions in the Subtropical South Pacific Ocean: comparison between in situ and predicted data. Biogeosciences 5:353-369. https://doi.org/10.5194/bg-5-353-2008.

Righetti, D., M. Vogt, N. Gruber, A. Psomas, and N. E. Zimmermann. 2019. Global pattern of phytoplankton diversity driven by temperature and environmental variability. Science Advances 5:eaau6253. https://doi.org/10.1126/sciadv.aau6253.

Segura, V., V. A. Lutz, A. Dogliotti, R. I. Silva, R. M. Negri, R. Akselman, and H. Benavides. 2013. Phytoplankton types and primary production in the Argentine Sea. Marine Ecology Progress Series 491:15-31. https://doi.org/10.3354/meps10461

Silva, R., R. Negri, and V. Lutz. 2009. Summer succession of ultraphytoplankton at the EPEA coastal station (Northern Argentina). Journal of Plankton Research 31:447-458. https://doi.org/10.1093/plankt/fbn128.

Simon, N., A.-L. Cras, E. Foulon, and R. Lemée. 2009. Diversity and evolution of marine phytoplankton. Comptes Rendus Biologies 332:159-170. https://doi.org/10.1016/j.crvi.2008.09.009.

Smetacek, V. 2001. A watery arms race. Nature 411:745. https://doi.org/10.1038/35081210.

Sommeria-Klein, G., R. Watteaux, F. M. Ibarbalz, J. J. P. Karlusich, D. Iudicone, C. Bowler, and H. Morlon. 2021. Global drivers of eukaryotic plankton biogeography in the sunlit ocean. Science 374:594-599. https://doi.org/10.1126/science.abb3717.

Sunagawa, S., S. G. Acinas, P. Bork, C. Bowler, D. Eveillard, G. Gorsky, L. Guidi, D. Iudicone, E. Karsenti, F. Lombard, H. Ogata, S. Pesant, M. B. Sullivan, P. Wincker, and C. de Vargas. 2020. Tara Oceans: towards global ocean ecosystems biology. Nature Reviews Microbiology 18:428-445.

Sunagawa, S., L. P. Coelho, S. Chaffron, J. R. Kultima, K. Labadie, et al. 2015. Structure and function of the global ocean microbiome. Science 348:1-10. https://doi.org/10.1126/science.1261359.

Thompson, G. A. 2004. Tintinnid diversity trends in the southwestern Atlantic Ocean (29 to 60 S). Aquatic Microbial Ecology 35:93-103. https://doi.org/10.3354/ame035093.

Thompson, G. A., E. O. Dinofrio, and V. A. Alder. 2013. Structure, abundance and biomass size spectra of copepods and other zooplankton communities in upper waters of the Southwestern Atlantic Ocean during summer. Journal of Plankton Research 35:610-629. https://doi.org/10.1093/plankt/fbt014.

Valla, D., A. R. Piola, C. S. Meinen, and E. Campos. 2018. Strong Mixing and Recirculation in the Northwestern Argentine Basin. Journal of Geophysical Research: Oceans 123:4624-4648. https://doi.org/10.1029/2018JC013907.

Van Heukelem, L., and C. S. Thomas. 2001. Computer-assisted high-performance liquid chromatography method development with applications to the isolation and analysis of phytoplankton pigments. Journal of Chromatography A 910:31-49. https://doi.org/10.1016/S0378-4347(00)00603-4.

Villar, E., G. K. Farrant, M. Follows, L. Garczarek, S. Speich, et al. 2015. Environmental characteristics of Agulhas rings affect interocean plankton transport. Science 348. https://doi.org/10.1126/science.1261447.

Vincent, F. J., S. Colin, S. Romac, E. Scalco, L. Bittner, Y. Garcia, R. M. Lopes, J. R. Dolan, A. Zingone, C. De Vargas, et al. 2018. The epibiotic life of the cosmopolitan diatom Fragilariopsis doliolus on heterotrophic ciliates in the open ocean. The ISME Journal 12:1094-1108. https://doi.org/10.1038/s41396-017-0029-1.

Yoder, J. A., and M. A. Kennelly. 2003. Seasonal and ENSO variability in global ocean phytoplankton chlorophyll derived from 4 years of SeaWiFS measurements. Global Biogeochemical Cycles 17. https://doi.org/10.1029/2002GB001942.

Zehr, J. P., J. B. Waterbury, P. J. Turner, J. P. Montoya, E. Omoregie, G. F. Steward, A. Hansen, and D. M. Karl. 2001. Unicellular cyanobacteria fix N2 in the subtropical North Pacific Ocean. Nature 412:635-638. https://doi.org/10.1038/35088063.